Aalto University School of Engineering
Department of Applied Mechanics

MEMO No CFD/MECHA-25-2012 DATE: November 14, 2012

TITLE

A study of an ogive shape projectile on the force and the momentum coefficients

AUTHOR(S)
Juhaveikko Ala-Juusela

ABSTRACT

A flow around projectile is simulated using computational fluid dynamics (CFD). Five ogive shapes are studied, three at two Mach numbers and two angles of attack and addional two at one Mach number and two angles of attack.

MAIN RESULT

A 100 mm cone increases a drag by less than 1%, a 250 mm cone up to 10% at $Ma = 2.0$.

PAGES
20

KEY WORDS
FINFLO, CFD, turbulence, SST $k - \omega$ model

APPROVED BY

Timo Siikonen November 14, 2012

Contents

1 Introduction

A flow over a projectile is simulated numerically using a FINFLO [1–3] flow solver. Five ogive shapes are studied in order to find out, how much aerodynamical force and momentum coefficients differ between ideally circular shape and shapes used in practice. Five geometries are investicated, two with the ogive shape formed by a rotation of a circular arc and three cases in which a part of the ogive section is replaced by a conical form.

In following, the turbulence model is firstly described, then simulation cases and grids are introduced and, finally, the results of the simulations are presented.

2 Flow Equations

A low-Reynolds number approach is used in FINFLO. The Reynolds-averaged Navier-Stokes equations, and the equations for the kinetic energy (k) and specific dissipation (ω) of turbulence can be written in the following form

$$\frac{\partial U}{\partial t} + \frac{\partial (F - F_v)}{\partial x} + \frac{\partial (G - G_v)}{\partial y} + \frac{\partial (H - H_v)}{\partial z} = Q \tag{1}$$

where the unknowns are $U = (\rho, \rho u, \rho v, \rho w, E, \rho k, \rho\omega)^T$. The inviscid fluxes are

$$F = \begin{pmatrix} \rho u \\ \rho u^2 + p + \frac{2}{3}\rho k \\ \rho v u \\ \rho w u \\ (E + p + \frac{2}{3}\rho k)u \\ \rho u k \\ \rho u \omega \end{pmatrix} G = \begin{pmatrix} \rho v \\ \rho u v \\ \rho v^2 + p + \frac{2}{3}\rho k \\ \rho w v \\ (E + p + \frac{2}{3}\rho k)v \\ \rho v k \\ \rho v \omega \end{pmatrix} H = \begin{pmatrix} \rho w \\ \rho u w \\ \rho v w \\ \rho w^2 + p + \frac{2}{3}\rho k \\ (E + p + \frac{2}{3}\rho k)w \\ \rho w k \\ \rho w \omega \end{pmatrix} \tag{2}$$

where ρ is the density, the velocity vector by using Cartesian components is $\vec{V} = u\vec{i} + v\vec{j} + w\vec{k}$, p is the pressure, k is the turbulent kinetic energy and ω its dissipation, and the total energy E is defined as

$$E = \rho e + \frac{\rho \vec{V} \cdot \vec{V}}{2} + \rho k \tag{3}$$

where e is the specific internal energy. The viscous fluxes are

$$F_v = \begin{pmatrix} 0 \\ \tau_{xx} \\ \tau_{xy} \\ \tau_{xz} \\ u\tau_{xx} + v\tau_{xy} + w\tau_{xz} - q_x \\ \mu_k(\partial k/\partial x) \\ \mu_\omega(\partial \omega/\partial x) \end{pmatrix} G_v = \begin{pmatrix} 0 \\ \tau_{xy} \\ \tau_{yy} \\ \tau_{yz} \\ u\tau_{xy} + v\tau_{yy} + w\tau_{yz} - q_y \\ \mu_k(\partial k/\partial y) \\ \mu_\omega(\partial \omega/\partial y) \end{pmatrix}$$

$$H_v = \begin{pmatrix} 0 \\ \tau_{xz} \\ \tau_{yz} \\ \tau_{zz} \\ u\tau_{xz} + v\tau_{yz} + w\tau_{zz} - q_z \\ \mu_k(\partial k/\partial z) \\ \mu_\omega(\partial \omega/\partial z) \end{pmatrix} \tag{4}$$

Here the stress tensor, τ_{ij}, includes laminar and turbulent components. The fluid is assumed to be Newtonian and, therefore, the laminar stresses are modelled by using Stokes hypothesis. The Reynolds stresses $\overline{\rho u_i'' u_j''}$ are included in the stress tensor τ_{ij}.

$$\tau_{ij} = \mu \left[\frac{\partial u_j}{\partial x_i} + \frac{\partial u_i}{\partial x_j} - \frac{2}{3}(\nabla \cdot \vec{V})\delta_{ij} \right] - \overline{\rho u_i'' u_j''} + \frac{2}{3}\rho k \delta_{ij} \tag{5}$$

For the Reynolds stresses, Boussinesq's approximation

$$-\overline{\rho u_i'' u_j''} = \mu_T \left[\frac{\partial u_j}{\partial x_i} + \frac{\partial u_i}{\partial x_j} - \frac{2}{3}(\nabla \cdot \vec{V})\delta_{ij} \right] - \frac{2}{3}\rho k \delta_{ij} \tag{6}$$

is utilized in RANS simulations. Here μ_T is a turbulent viscosity coefficient, which is calculated by using a turbulence model, and δ_{ij} is the Kronecker's delta. In the momentum and energy equations, the kinetic energy contribution $2/3\rho k\delta_{ij}$ has been connected with pressure and appears in the convective fluxes, whereas the diffusive part is connected with the viscous fluxes. The viscous stresses contains a laminar and a turbulent parts. The heat flux can be written as

$$\vec{q} = -(\lambda + \lambda_T)\nabla T = -\left(\mu \frac{c_p}{Pr} + \mu_T \frac{c_p}{Pr_T} \right) \nabla T \tag{7}$$

where λ is a molecular and λ_T a turbulent thermal conductivity coefficient and Pr is a laminar and Pr_T a turbulent Prandtl number, and c_p is a specific heat at constant pressure. The diffusion of turbulence variables is modelled as

$$\mu_k \nabla k = \left(\mu + \frac{\mu_T}{\sigma_k} \right) \nabla k \tag{8}$$

$$\mu_\omega \nabla \omega = \left(\mu + \frac{\mu_T}{\sigma_\omega} \right) \nabla \omega \tag{9}$$

where σ_k and σ_ω are turbulent Schmidt numbers of k and ω, respectively. Density is obtained from an equation of state $\rho = \rho(p, T)$ Since the case for the ogive cylinder is incompressible, pressure differences $p - p_0$ are solved instead of pressure. The components of the source term Q are non-zero in possible buoyancy terms and in turbulence model equations.

3 SST $k-\omega$ RANS-model

The model equations using an implicit summation over j-index are

$$\begin{aligned} \rho\frac{\partial k}{\partial t}+\rho u_j\frac{\partial k}{\partial x_j} &= P-\beta^*\rho k\omega \\ &+ \frac{\partial}{\partial x_j}\left[(\mu+\frac{\mu_T}{\sigma_k})\frac{\partial k}{\partial x_j}\right] \end{aligned} \tag{10}$$

$$\begin{aligned} \rho\frac{\partial \omega}{\partial t}+\rho u_j\frac{\partial \omega}{\partial x_j} &= \frac{\gamma\rho}{\mu_T}P-\beta\rho\omega^2 \\ &+ \frac{\partial}{\partial x_j}\left[(\mu+\frac{\mu_T}{\sigma_\omega})\frac{\partial \omega}{\partial x_j}\right] \\ &+ 2\rho\frac{1-F_1}{\sigma_{\omega 2}\omega}\frac{\partial k}{\partial x_j}\frac{\partial \omega}{\partial x_j} \end{aligned} \tag{11}$$

The model coefficients in Eqs. (10) and (11) are obtained from

$$(\sigma_k\ \sigma_\omega\ \beta)^T = F_1\,(\sigma_k\ \sigma_\omega\ \beta)_1^T + (1-F_1)\,(\sigma_k\ \sigma_\omega\ \beta)_2^T \tag{12}$$

with the following values

$$\begin{array}{lll} \sigma_{k1} = 1.176 & \sigma_{\omega 1} = 2.0 & \beta_1 = 0.075 \\ \sigma_{k2} = 1.0 & \sigma_{\omega 2} = 1.168 & \beta_2 = 0.0828 \end{array}$$

Coefficients κ and β^* have constant values of 0.41 and 0.09. Coefficient γ is calculated from

$$\gamma = \frac{\beta}{\beta^*} - \frac{\kappa^2}{\sigma_\omega\sqrt{\beta^*}} \tag{13}$$

Term P in Eqs. (10) and (11) is the production of turbulent kinetic energy and calculated using the Boussinesq approximation from Eq. (6). The last term in the ω-equation originates from the transformed ϵ-equation and it is called a cross-diffusion term. The switching function which governs the choice between the ω- and the ϵ-equations is

$$F_1 = \tanh\left(\Gamma^4\right) \tag{14}$$

where

$$\Gamma = \min\left(\max\left(\frac{\sqrt{k}}{\beta^*\omega d};\frac{500\nu}{\omega d^2}\right);\frac{4\rho\sigma_{\omega 2}k}{CD_{k\omega}d^2}\right) \tag{15}$$

The first term is a turbulent length scale divided with the distance from the walls (d). This ratio is around 2.5 in a logarithmic layer and approaches zero in an outer layer. The second term has a value of ≥ 1 only in a viscous sublayer.

The meaning of the third term is to ensure stable behaviour of F_1 when the value of ω in the free stream is small. It utilizes a parameter

$$CD_{k\omega} = \max\left(\frac{2\rho}{\sigma_{\omega 2}\omega}\frac{\partial k}{\partial x_j}\frac{\partial \omega}{\partial x_j}; CD_{k\omega\,\min}\right) \tag{16}$$

which is a lower limit of the cross diffusion term. The main purpose of the switching function is to limit the use of the $k-\omega$ model into the boundary layer region. The switch is naturally a weak point in the model, but it seems to work at least in cases of external flows.

4 Computational Domains, Grids and Boundary Conditions

The case is an axisymmetrical projectile with a blunt head followed by an ogive section connected to a cyliderical base. The ogive is 465 mm and the base section 500 mm long. A head diameter is 18 mm and the base diameter is 155 mm.

Five ogive geometries are simulated. Two baseline geometries are formed by a circular arc in an axial direction. In alternative geometries circular shape is replaced in the front part of the ogive by the cone. In geometries 1, 2 and 3 the radius of the arc is twice the circular arc which unites tangentially to the base side. The cross-section of the arcs and midline of the projectile is the same in front of the head. The cone is either 100 mm or 250 mm long. In geometries 4 and 5 the radius is a circular arc which unites tangentially to the base side. The cone is 250 mm long. Geometries 1, 2 and 3 are shown in Fig. 1. and geometries 4 and 5 in Fig. 2.

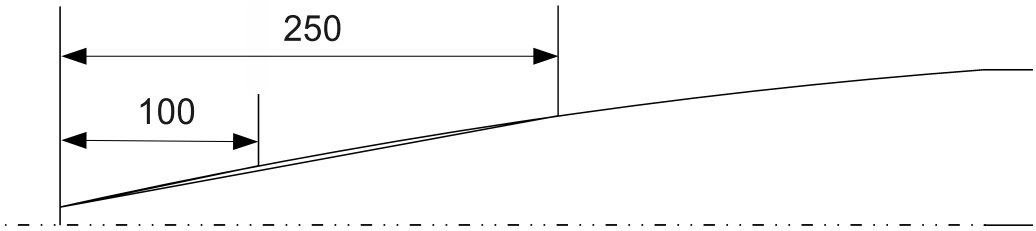

Fig. 1: A geometric layout of the projectile. Geometries 1, 2 and 3.

A structured grid applied consists of two blocks and it has totally 259 776 cells. A singularity is removed from otherwise a rotational grid. In that way the grid can also be used with computational code using an un-structured grid. Due to the symmetry, a half of the projectile is modelled. The blunt end of the base is not modelled, but the outlet is placed directly at the end of the base. The grid extends 70 chord lenghts in front and sides of the projectile. The surface grid and the grid on a symmetry plane are shown in Fig. 3.

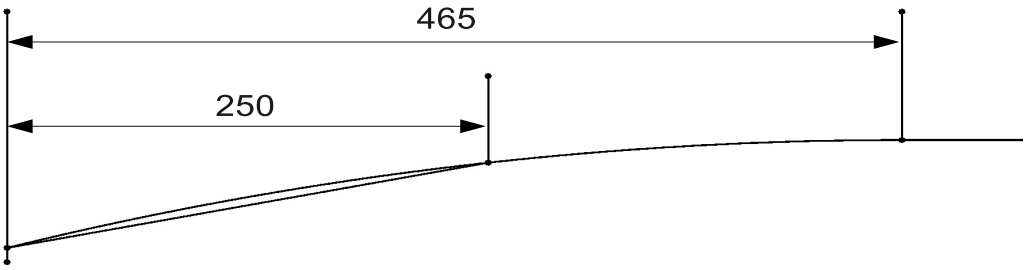

Fig. 2: A geometric layout of the projectile. Geometries 4 and 5.

As boundary conditions, velocity and turbulence quantities are given at the far field, pressure is given at the outlet. However, in a case $Ma > 1$ the pressure does not affect upstream except inside the boundary layer.

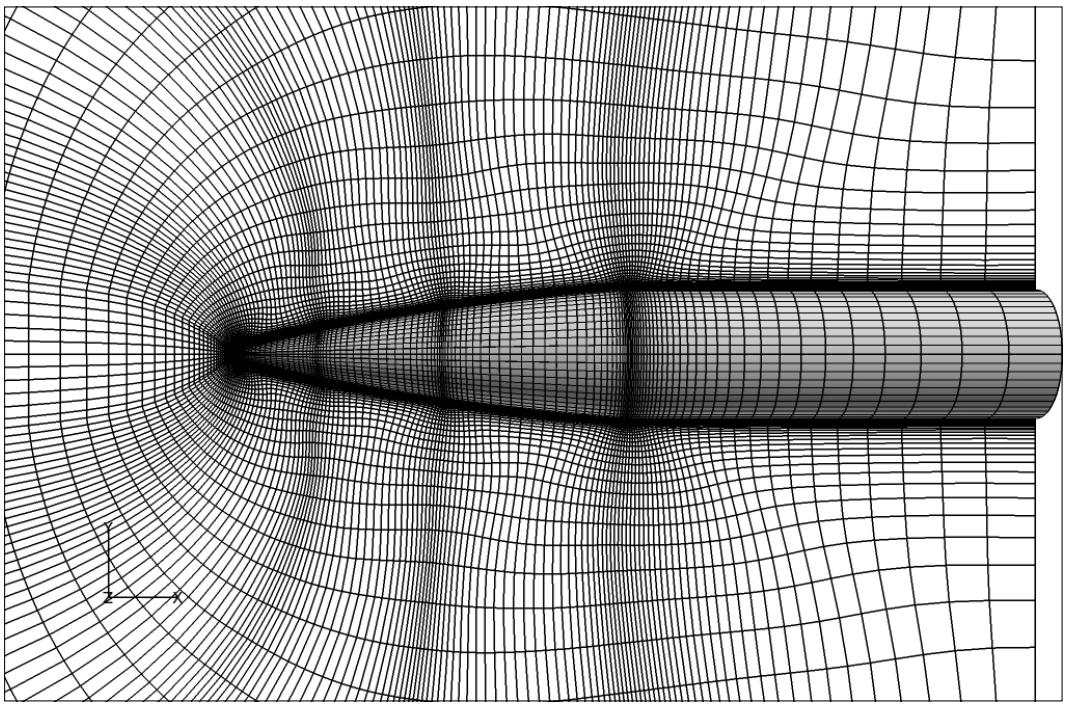

Fig. 3: The computational grid at symmetry plane and on the surface of the projectile.

5 Results

5.1 Geometries 1, 2 and 3

These cases are simulated with the SST k-ω turbulence model. Two Mach numbers, $Ma = 0.5$ and $Ma = 2.0$, are used at two angles of attack $\alpha = 0°$ and $\alpha = 3°$. Pressure distributions on the surface of projectile and at the symmetry plane of all geometries at $Ma = 2.0$ and at an angle of attack 3° are shown in Figs. 4 – 6.

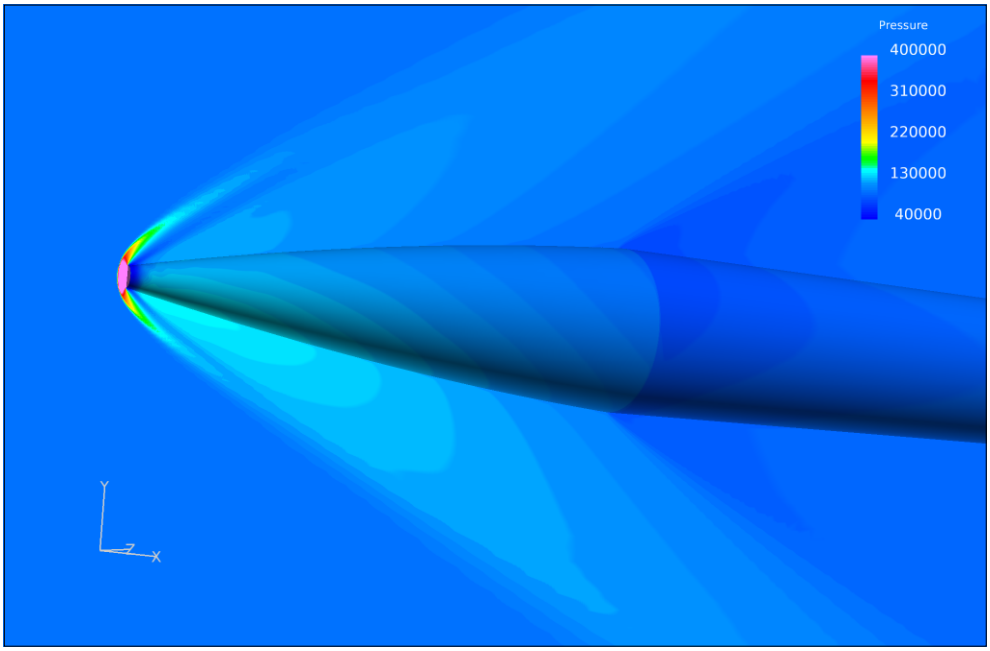

Fig. 4: Distributions of the pressure on the surface of the projectile and at the symmetry plane of geometry 1. The Mach number is 2.0 and the angle of attack 3°.

Distributions of a pressure coefficient along the surface of the projectile at cross sections at a top, midline and bottom and similar distributions of the friction coefficient are given in Figs. 7 – 10. At the angle of attack 0° the distribution is taken along the midline of the projectile, at the angle of attack 3° also along the lines on the top and on the bottom of the projectile. Discontinuities of the surface shape can be seen clearly from the pressure and friction coefficient curves.

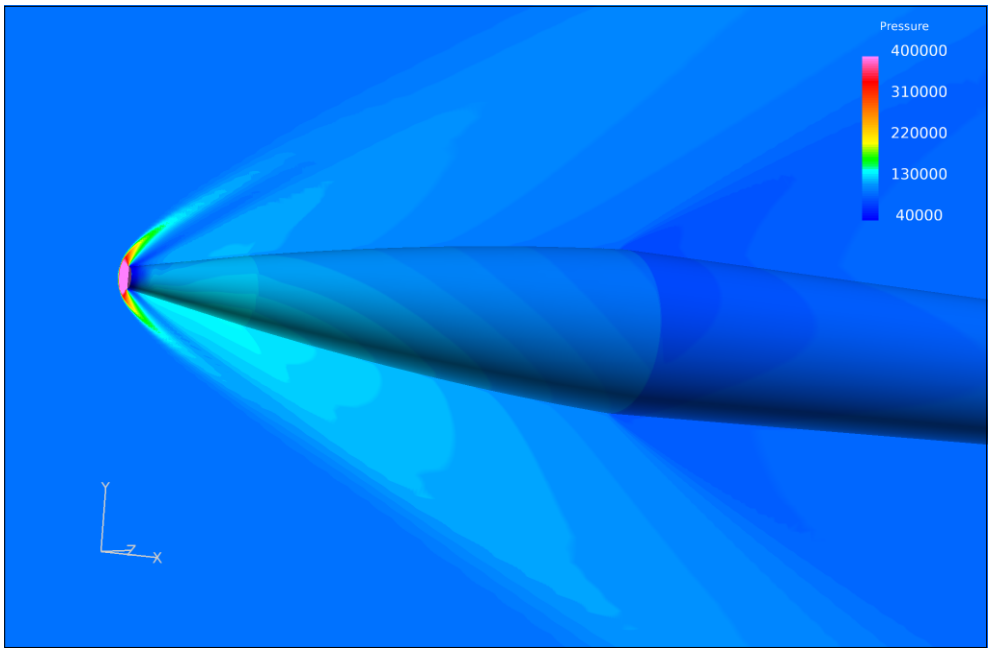

Fig. 5: Distributions of the pressure on the surface of the projectile and at the symmetry plane of the geometry 2. The Mach number is 2.0 and the angle of attack 3°.

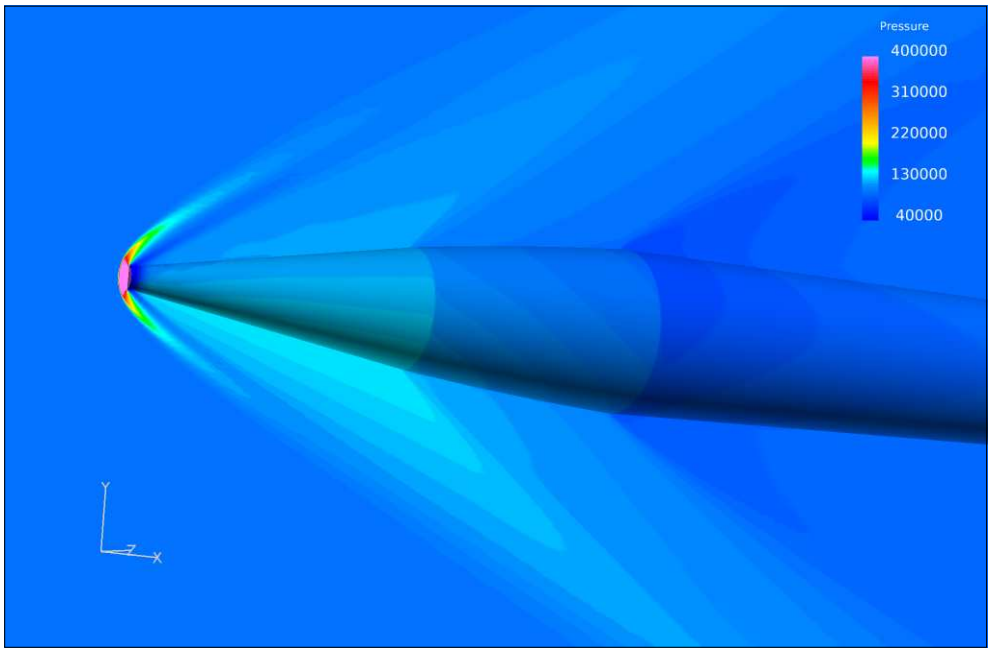

Fig. 6: Distributions of the pressure on the surface of the projectile and at the symmetry plane of the geometry 3. The Mach number is 2.0 and the angle of attack 3°.

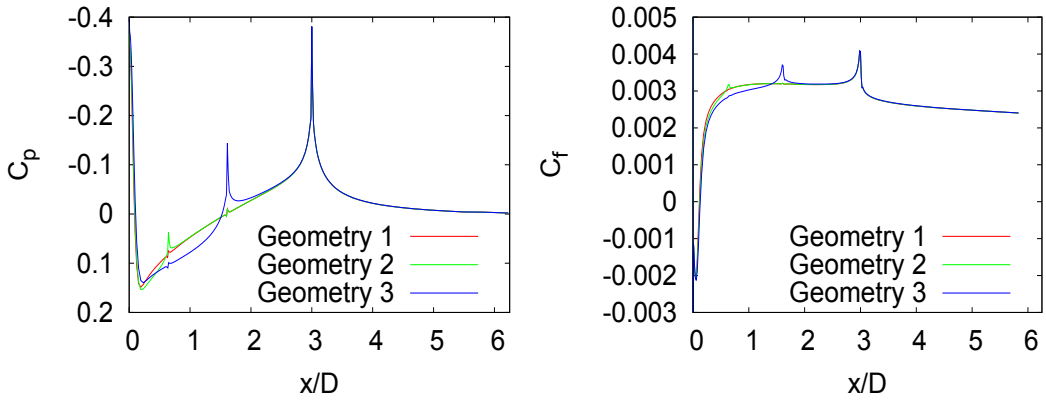

Fig. 7: Distributions of the pressure coefficient (left) and the friction coefficient (right) along the projectile at midline. The Mach number is 0.5 and the angle of attack 0°.

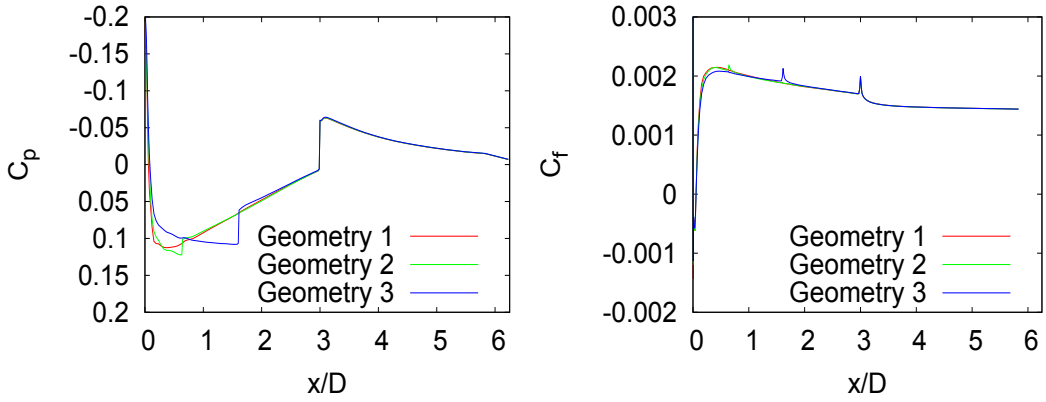

Fig. 8: Distributions of the pressure coefficient (left) and the friction coefficient (right) along the projectile at midline. The Mach number is 2.0 and the angle of attack 0°.

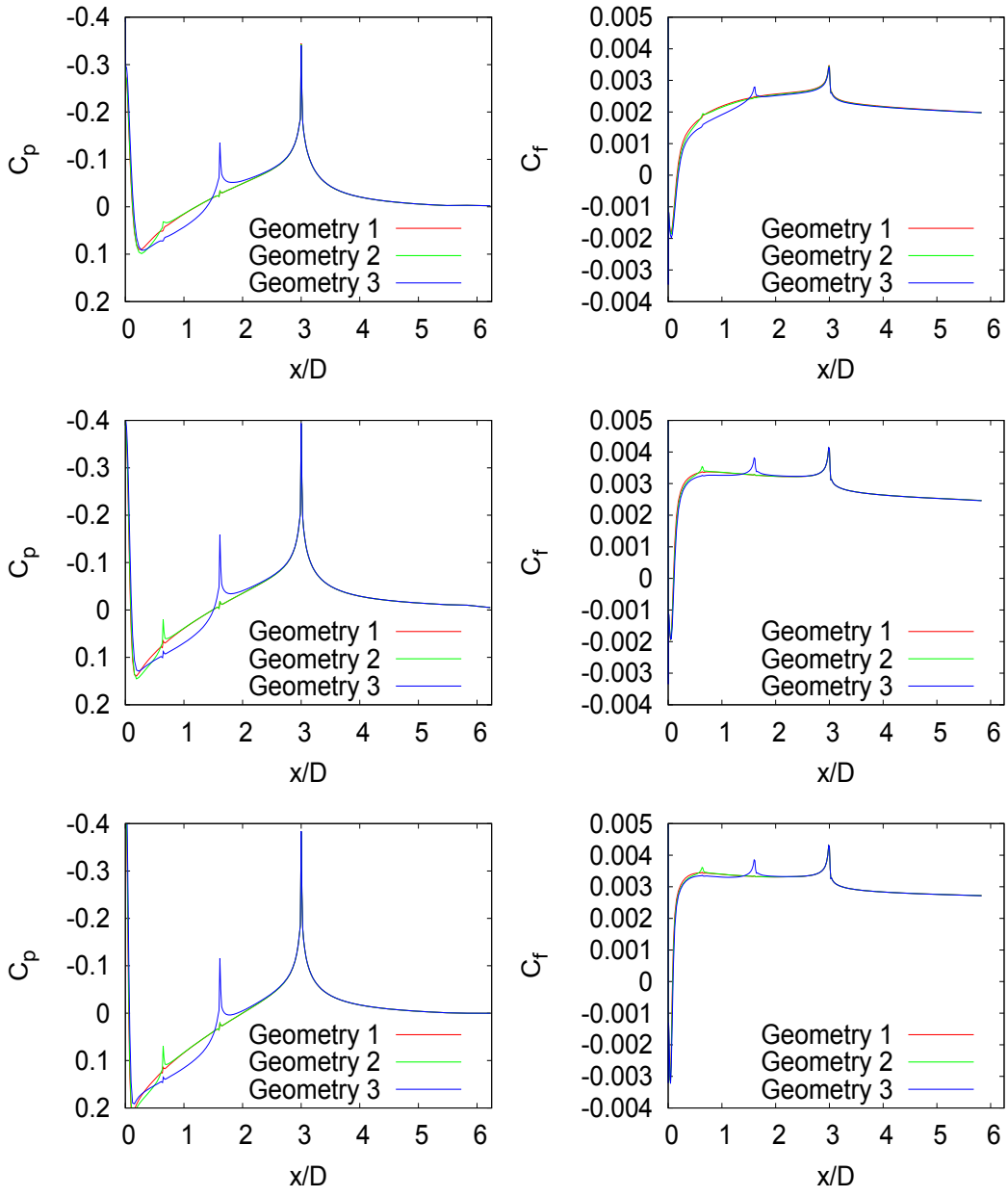

Fig. 9: Distributions of the pressure coefficient (left) and the friction coefficient (right) along the projectile at midline. The Mach number is 0.5 and the angle of attack 3°.

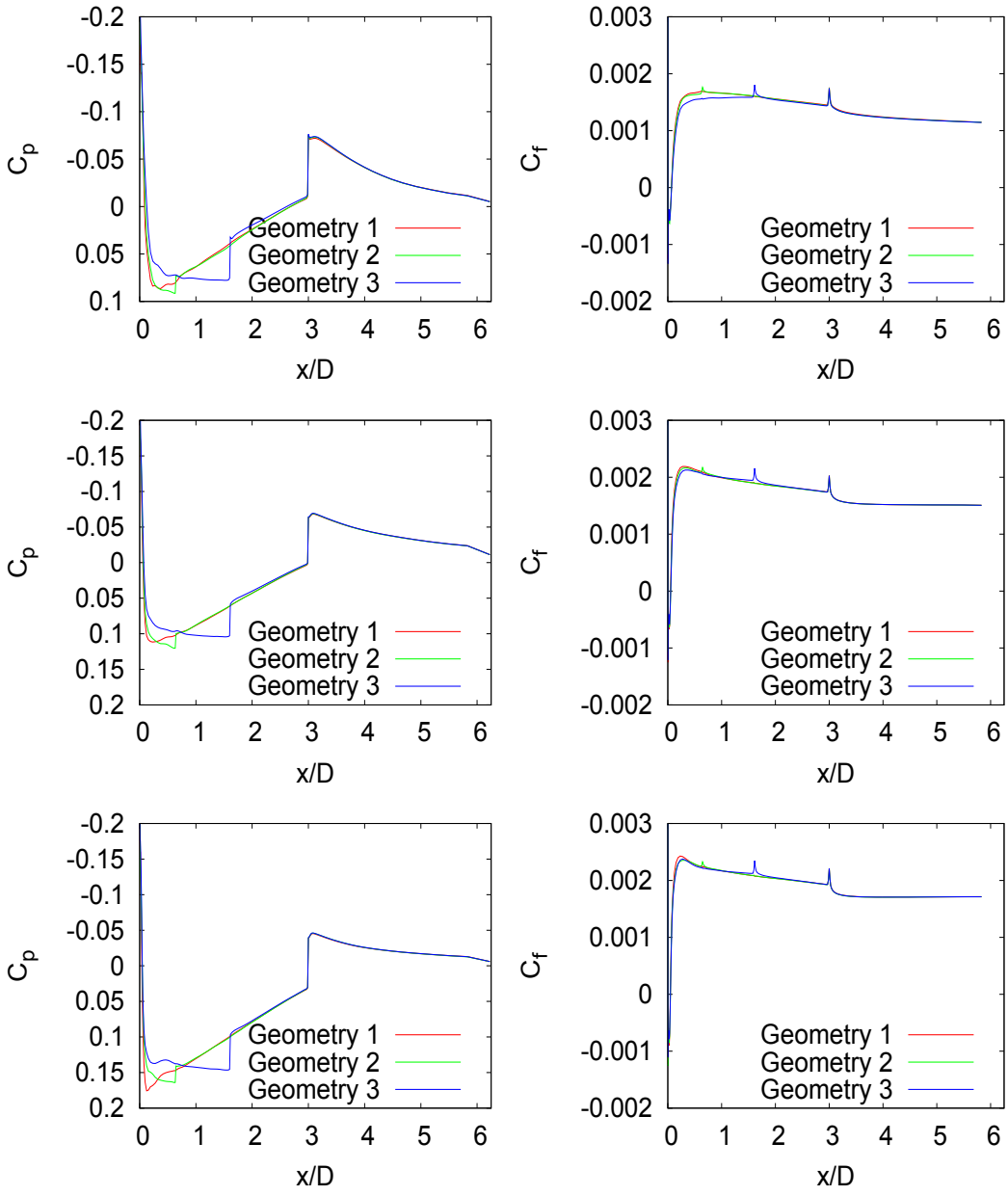

Fig. 10: Distributions of the pressure coefficient (left) and the friction coefficient (right) along the projectile at midline. The Mach number is 2.0 and the angle of attack 3°.

Drag, lift and momentum coefficiets are shown in Tables 1 – 4. As a comparison, values of totally conical ogive shape is presented for cases of $Ma = 2.0$. Also the ratio of coefficients as compared to geometry 1 is presented in the tables. A center of the momentum is in a head of the projectile ($x = 0\,\mathrm{mm}$). A reference area for the forces is $\pi d^2/4$ and a reference length for the momentum is a diameter ($d = 155\,\mathrm{mm}$).

At a Mach number of $Ma = 0.5$ the total drag coefficient is increased less than 1% with geometry 2 and around 1.5% with geometry 3. At the Mach number of $Ma = 2.0$ the drag is on about the same level with geometry 2, but increases 2.5 - 3 % with geometry 3. It should be noted that the real accuracy of the computations is less than the six decimal places given in the tables. The figures are given accurately in order to facilitate a comparison of the simulated coefficients in a case of small differences.

Table. 1: Drag, lift and momentum coeffcients, $Ma = 0.5$, $\alpha = 0°$

Case	C_D	$C_D/C_{D,g.\ 1}$	C_F	$C_F/C_{F,g.\ 1}$	C_m	$C_m/C_{m,g.\ 1}$
Total						
Geom. 1	0.064756	1.000000	0.000056	1.000000	0.000136	1.000000
Geom. 2	0.065027	1.004180	0.000094	1.695131	0.000178	1.314017
Geom. 3	0.065254	1.007692	0.000095	1.701733	0.000167	1.232490
Ogive						
Geom. 1	0.031777	1.000000	0.000041	1.000000	0.000068	1.000000
Geom. 2	0.032042	1.008320	0.000084	2.023457	0.000134	1.984461
Geom. 3	0.032228	1.014164	0.000090	2.164834	0.000148	2.182777
Base						
Geom. 1	0.032978	1.000000	0.000014	1.000000	0.000068	1.000000
Geom. 2	0.032985	1.000191	0.000011	0.746174	0.000044	0.646425
Geom. 3	0.033026	1.001455	0.000005	0.363237	0.000019	0.286246

Table. 2: Drag, lift and momentum coeffcients $Ma = 0.5$, $\alpha = 3°$

Case	C_D	$C_D/C_{D,g.\ 1}$	C_F	$C_F/C_{F,g.\ 1}$	C_m	$C_m/C_{m,g.\ 1}$
Total						
Geom. 1	0.068218	1.000000	0.108371	1.000000	0.217515	1.000000
Geom. 2	0.068483	1.003885	0.108421	1.000461	0.217651	1.000625
Geom. 3	0.068649	1.006319	0.10837	0.999991	0.220732	1.014790
Ogive						
Geom. 1	0.034417	1.000000	0.096728	1.000000	0.159598	1.000000
Geom. 2	0.034683	1.007746	0.096787	1.000616	0.159752	1.000965
Geom. 3	0.034884	1.013584	0.096656	0.999265	0.162485	1.018089
Base						
Geom. 1	0.033801	1.000000	0.011643	1.000000	0.057917	1.000000
Geom. 2	0.033800	0.999953	0.011634	0.999227	0.057899	0.999689
Geom. 3	0.033765	0.998923	0.011714	1.006133	0.058247	1.005700

Table. 3: Drag, lift and momentum coeffcients $Ma = 2.0$, $\alpha = 0°$

Case	C_D	$C_D/C_{D,g.\ 1}$	C_F	$C_F/C_{F,g.\ 1}$	C_m	$C_m/C_{m,g.\ 1}$
Total						
Geom. 1	0.113046	1.000000	-0.000355	1.000000	0.000462	1.000000
Geom. 2	0.113106	1.000525	0.001107	-3.118310	0.002558	5.540829
Geom. 3	0.115943	1.025625	-0.000337	0.949296	0.000127	0.275748
Conical	0.124904	1.104896	-0.000466	1.328037	-0.000823	-1.782715
Ogive						
Geom. 1	0.094035	1.000000	-0.000851	1.000000	-0.001581	1.000000
Geom. 2	0.094104	1.000733	0.000573	-0.673408	0.000640	-0.404605
Geom. 3	0.096933	1.030818	-0.000368	0.432306	-0.000552	0.349172
Conical	0.105860	1.125750	-0.000447	0.525076	-0.000621	0.392801
Base						
Geom. 1	0.019011	1.000000	0.000500	1.000000	0.002043	1.000000
Geom. 2	0.019002	0.999495	0.000546	1.092841	0.001919	0.939184
Geom. 3	0.019010	0.999937	0.000033	0.065310	0.000679	0.332577
Conical	0.019044	1.001746	-0.000019	-0.038365	-0.000202	-0.098909

Table. 4: Drag, lift and momentum coeffcients $Ma = 2.0$, $\alpha = 3°$

Case	C_D	$C_D/C_{D,g.\ 1}$	C_F	$C_F/C_{F,g.\ 1}$	C_m	$C_m/C_{m,g.\ 1}$
Total						
Geom. 1	0.123118	1.000000	0.135232	1.000000	0.310509	1.000000
Geom. 2	0.123013	0.999153	0.134237	0.992642	0.309617	0.997127
Geom. 3	0.126362	1.026353	0.134797	0.996783	0.315217	1.015162
Conical	0.131677	1.069520	0.132822	0.982177	0.348806	1.123336
Ogive						
Geom. 1	0.101999	1.000000	0.103364	1.000000	0.189637	1.000000
Geom. 2	0.101926	0.999284	0.102611	0.992715	0.189587	0.999736
Geom. 3	0.105249	1.031863	0.102786	0.994408	0.194151	1.023803
Conical	0.110003	1.078471	0.091272	0.883018	0.188223	0.992544
Base						
Geom. 1	0.021119	1.000000	0.031868	1.000000	0.120872	1.000000
Geom. 2	0.021087	0.998518	0.031626	0.992425	0.120030	0.993034
Geom. 3	0.021113	0.999740	0.032011	1.004500	0.121066	1.001605
Conical	0.021674	1.026285	0.041549	1.303802	0.160583	1.328538

5.2 Geometries 4 and 5

Also these cases are simulated with the SST k-ω turbulence model. Mach number $Ma = 2.0$ is used at two angles of attack $\alpha = 0°$ and $\alpha = 3°$. Pressure distributions on the surface of projectile and at the symmetry plane of all geometries at $Ma = 2.0$ and at an angle of attack 3° are shown in Figs. 11 – 12.

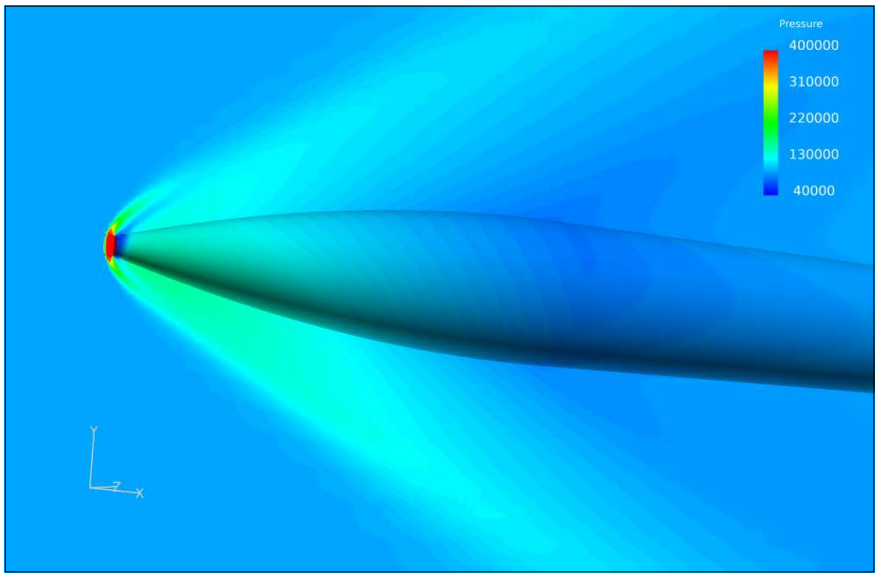

Fig. 11: Distributions of the pressure on the surface of the projectile and at the symmetry plane of geometry 4. The Mach number is 2.0 and the angle of attack 3°.

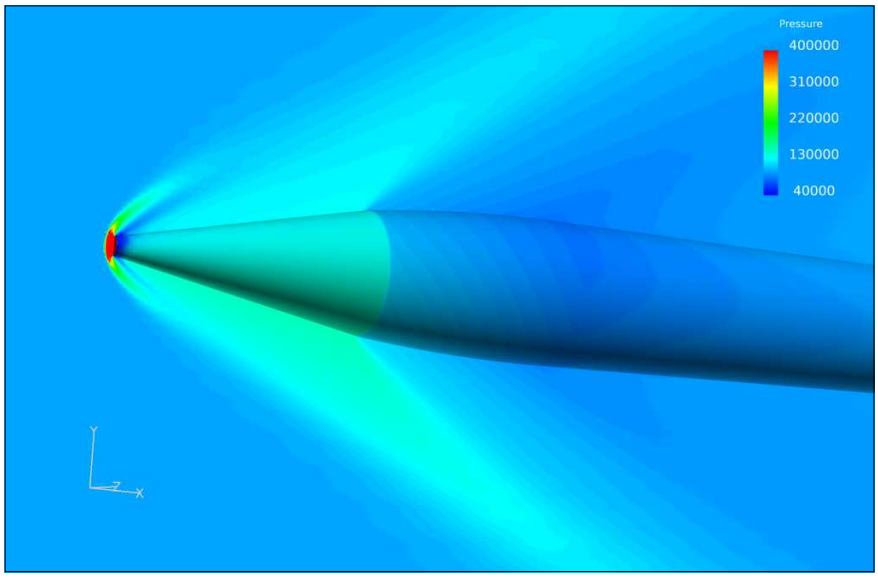

Fig. 12: Distributions of the pressure on the surface of the projectile and at the symmetry plane of the geometry 5. The Mach number is 2.0 and the angle of attack 3°.

Distributions of a pressure coefficient along the surface of the projectile at cross sections at a top, midline and bottom and similar distributions of the friction coefficient are given in Fig. 13 – 14. At the angle of attack 0° the distribution is taken along the midline of the projectile, at the angle of attack 3° also along the lines on the top and on the bottom of the projectile. Again, discontinuties of the surface shape can be seen clearly from the pressure and friction coefficient curves.

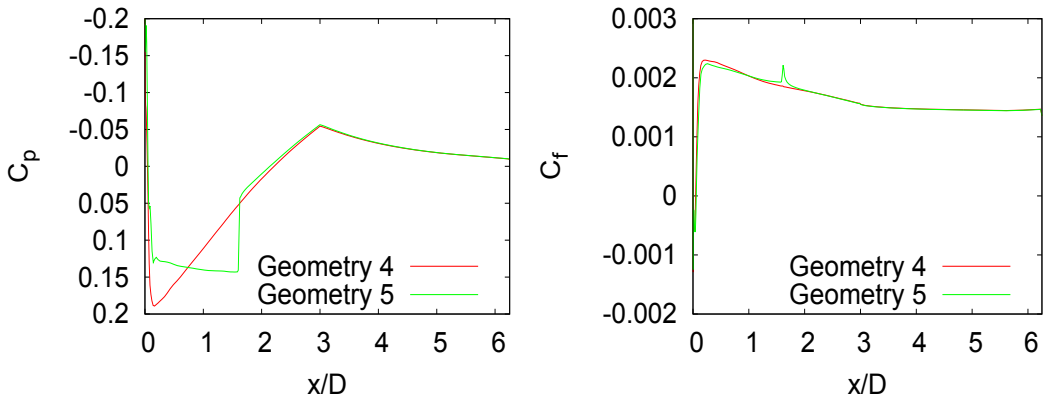

Fig. 13: Distributions of the pressure coefficient (left) and the friction coefficient (right) along the projectile at midline. The Mach number is 2.0 and the angle of attack 0°.

Drag, lift and momentum coefficiets are shown in Tables 5 – 6. As a comparison, values of totally conical ogive shape is presented. Also the ratio of coefficients as compared to geometry 4 is presented in tables. As in the previous cases a center of the momentum is in a head of the projectile ($x = 0\,\text{mm}$). A reference area for the forces is $\pi d^2/4$ and a reference length for the momentum is a diameter ($d = 155\,\text{mm}$). In the ogive section the drag increases almost 10 % and momentum almost 5 % with geometry 5.

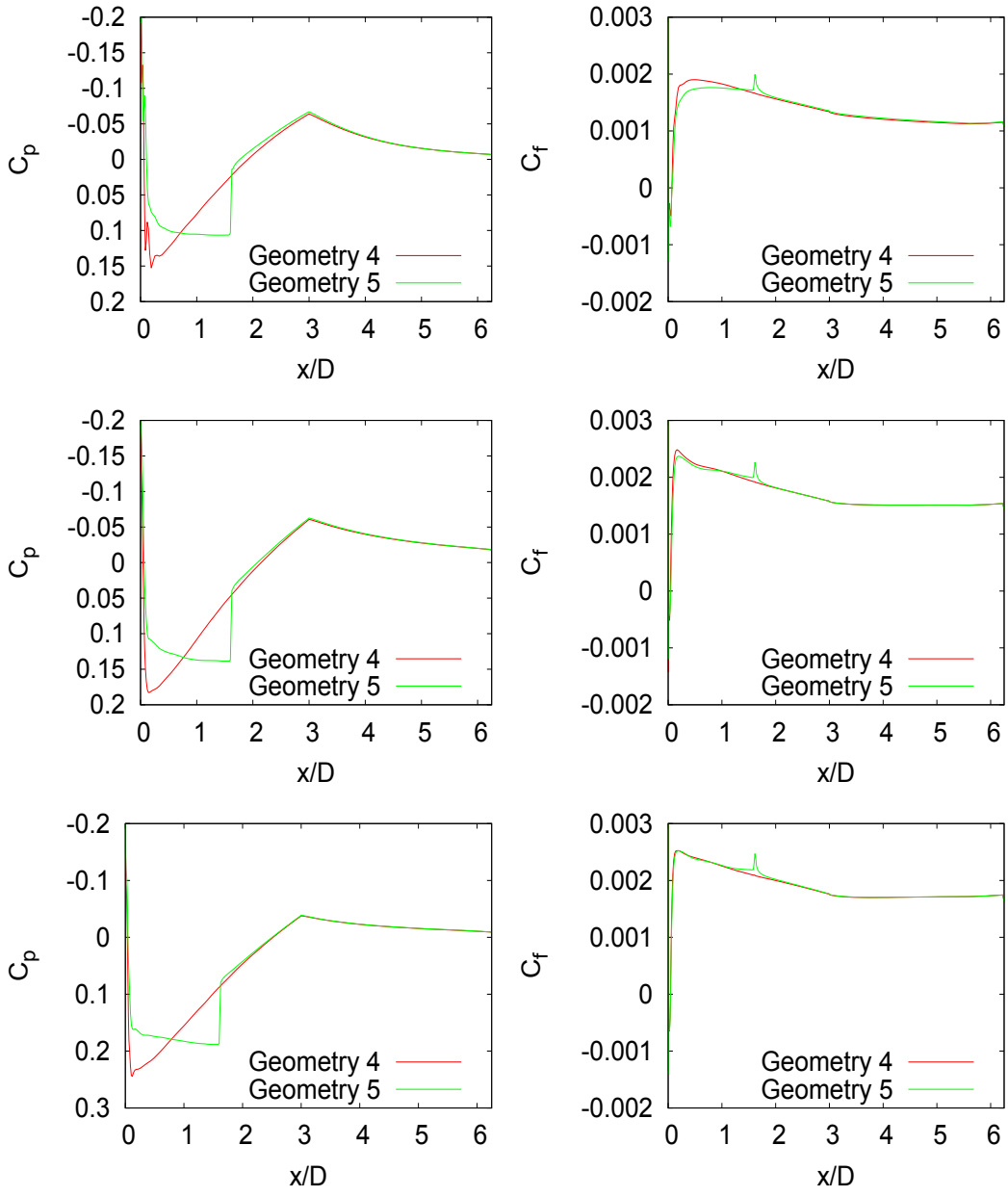

Fig. 14: Distributions of the pressure coefficient (left) and the friction coefficient (right) along the projectile at midline. The Mach number is 2.0 and the angle of attack 3°.

Table. 5: Drag, lift and momentum coeffcients $Ma = 2.0$, $\alpha = 0°$

Case	C_D	$C_D/C_{D,g.\ 4}$	C_F	$C_F/C_{F,g.\ 4}$	C_m	$C_m/C_{m,g.\ 4}$
Total						
Geom. 4	0.121293	1.000000	0.000283	1.000000	0.000180	1.000000
Geom. 5	0.131165	1.081388	-0.000462	-1.632786	-0.001494	-8.286095
Conical	0.124904	1.029770	-0.000466	-1.645637	-0.000823	-4.564163
Ogive						
Geom. 4	0.102347	1.000000	0.000336	1.000000	0.000182	1.000000
Geom. 5	0.112263	1.096886	-0.000211	-0.627856	-0.000406	-2.228249
Conical	0.105860	1.034324	-0.000447	-1.329943	-0.000621	-3.407197
Base						
Geom. 4	0.018946	1.000000	-0.000053	1.000000	-0.000002	1.000000
Geom. 5	0.018902	0.997667	-0.000251	4.762472	-0.001088	562.075
Conical	0.019044	1.005167	-0.000019	0.363403	-0.000202	104.367162

Table. 6: Drag, lift and momentum coeffcients $Ma = 2.0$, $\alpha = 3°$

Case	C_D	$C_D/C_{D,g.\ 4}$	C_F	$C_F/C_{F,g.\ 4}$	C_m	$C_m/C_{m,g.\ 4}$
Total						
Geom. 4	0.128465	1.000000	0.136178	1.000000	0.259607	1.000000
Geom. 5	0.138172	1.075566	0.136516	1.002484	0.274884	1.058847
Conical	0.131677	1.025004	0.132822	0.975355	0.348806	1.343592
Ogive						
Geom. 4	0.108250	1.000000	0.118519	1.000000	0.197960	1.000000
Geom. 5	0.117862	1.088794	0.117142	0.988382	0.207297	1.047166
Conical	0.110003	1.016194	0.091272	0.770107	0.188223	0.950813
Base						
Geom. 4	0.020215	1.000000	0.017659	1.000000	0.061647	1.000000
Geom. 5	0.020310	1.004729	0.019374	1.097131	0.067587	1.096357
Conical	0.021674	1.072181	0.041549	2.352908	0.160583	2.604879

6 Conclusions

The effect of the axisymmetric projetile ogive shape is studied by simulating five different ogive geometries. Two ogive forms, created by rotating a circular arc, are in three cases replaced partly by conical shape, a cone, either 100 mm or 250 mm long. The shorter cone increases drag less than 1%, the longer one up to 3% at $Ma = 2.0$ in the case of longer arc radius and up to almost 10% at $Ma = 2.0$ in the case of shorter arc radius.

References

[1] *FINFLO User Guide, version 8.2.* Helsinki University of Technology, Finland, 2010.

[2] *FINFLO User Guide, version 7.1.* Helsinki University of Technology, Finland, 2003.

[3] Siikonen, T., "Laskennallisen virtausmekaniikan ja lämmönsiirron jatkoopintojakso," Teknillinen korkeakoulu, Sovelletun termodynamiikan laboratorio, Espoo, 1998.